



## Botulinum neurotoxin serotype A inhibitors: Small-molecule mercaptoacetamide analogs

Scott T. Moe<sup>a</sup>, Andrew B. Thompson<sup>a</sup>, Genessa M. Smith<sup>a,†</sup>, Ross A. Fredenburg<sup>b,‡</sup>,  
Ross L. Stein<sup>b</sup>, Alan R. Jacobson<sup>a,\*</sup>

<sup>a</sup> Absolute Science, Inc., Lexington, MA 02421, United States

<sup>b</sup> Laboratory for Drug Discovery in Neurodegeneration, Brigham & Women's Hospital, Cambridge, MA 02139, United States

### ARTICLE INFO

#### Article history:

Received 16 January 2009

Revised 5 March 2009

Accepted 6 March 2009

Available online 14 March 2009

#### Keywords:

Botulism

Botulinum

BoNT/A

Metalloprotease inhibitors

Mercaptoacetamides

### ABSTRACT

Botulinum neurotoxin elicits its paralytic activity through a zinc-dependant metalloprotease that cleaves proteins involved in neurotransmitter release. Currently, no drugs are available to reverse the effects of botulinum intoxication. Herein we report the design of a novel series of mercaptoacetamide small-molecule inhibitors active against botulinum neurotoxin serotype A. These analogs show low micromolar inhibitory activity against the isolated enzyme. Structure–activity relationship studies for a series of mercaptoacetamide analogs of 5-amino-3-phenylpyrazole reveal components essential for potent inhibitory activity.

© 2009 Elsevier Ltd. All rights reserved.

## 1. Introduction

*Clostridium botulinum* bacteria cause botulism, a life-threatening disease. The bacteria produce several proteinaceous botulinum toxins, categorized into seven distinct serotypes (A–G). Despite its widespread medicinal use, botulinum neurotoxin serotype A (BoNT/A) is extremely toxic, showing an LD<sub>50</sub> in humans of 1 ng/kg, making it the most poisonous naturally occurring substance known.<sup>1,2</sup> The relative ease of obtaining the neurotoxin coupled with its potential use as a bioterrorist weapon,<sup>3,4</sup> has galvanized research in the field in an effort to discover therapeutic agents against the toxin.<sup>5</sup>

BoNT/A is a protein comprised of a light chain (LC) and a heavy chain (HC) that are held together through a single disulfide bond. While the HC is responsible for the transport of the toxin into the cell,<sup>6</sup> it is the LC that is responsible for the observed toxic effects through its action as a zinc metalloprotease. Because of this mechanism of toxicity, the use of antibodies has an extremely narrow window of opportunity to neutralize the toxin, and hence the importance of discovering small-molecule inhibitors of the LC that

can prevent and/or reverse intoxication after the toxin has entered the cell.

The LC cleaves SNARE (Soluble N-ethylmaleimide-Sensitive factor Attachment protein REceptor) proteins, specifically SNAP-25 (synaptosome-associate protein, 25 kDa), resulting in the inhibition of acetylcholine release from the nerve cell.<sup>7,8</sup> The resulting flaccid paralysis can ultimately lead to death of the infected patient by causing either cardiac arrest or respiratory failure. Though an intoxicated patient can generally recover if kept on a ventilator for the duration of the paralysis, treatment can last for months.<sup>9</sup> In the event of a large outbreak, this would be a nonviable treatment option for large numbers of people.

Initial studies of inhibitors of the BoNT/A LC were peptide-based and designed around the known cleavage site of the SNAP-25 protein. Seminal work by Schmidt<sup>10,11</sup> and Rich<sup>12–15</sup> found that the cysteine-containing peptide CRATKML (**1**, Fig. 1) inhibited BoNT/A with a K<sub>i</sub> of 2 μM. However, Schmidt's group showed that truncation to the tetrapeptide resulted in a 20-fold loss of inhibitory activity.<sup>16</sup> While these materials serve as excellent research tools, their physicochemical and pharmacokinetic properties make them unlikely candidates as therapeutic agents.

Despite decades of intensive investigation to find small-molecule inhibitors of the BoNT/A LC, only recently has Janda reported the first discovery of small-molecule hydroxamic acids as potent inhibitors of the enzyme.<sup>17,18</sup> The most active analog, 2,4-dichlorocinnamic hydroxamic acid (**2**), is the most potent small-molecule inhibitor of BoNT/A reported to date, showing a K<sub>i</sub> = 0.3 μM.

\* Corresponding author. Address: Absolute Science, Inc., PO Box 382366, Cambridge, MA 02238, United States. Tel./fax: +1 781 676 0010.

E-mail address: [arj@absolutescience.com](mailto:arj@absolutescience.com) (A.R. Jacobson).

<sup>†</sup> Present address: Colorado State University, Department of Chemistry, Ft. Collins, CO 80523, United States.

<sup>‡</sup> Present address: Link Medicine Corporation, 161 First Street, Cambridge, MA 02142, United States.

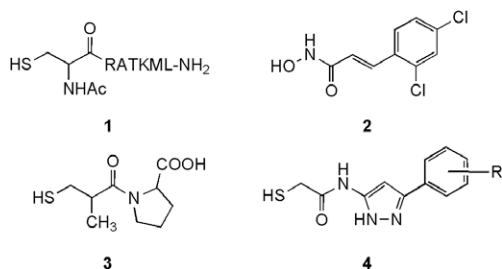


**Figure 1.** Botulinum neurotoxin serotype A inhibitors: Structural comparison with the metalloprotease inhibitor drug captopril **3**.

## 2. Results and discussion

Our initial design process for the development of inhibitors against the LC was based on an amalgamation of captopril, (S)-1-(3-mercapto-2-methyl-1-oxopropyl)-L-proline (**3**), an angiotensin converting enzyme (ACE)<sup>19</sup> inhibitor, Schmidt's CRATKML (**1**) and the small-molecule inhibitor (**2**) reported by Janda's group.<sup>17,18</sup> Given the known propensity of sulfur as well as hydroxamic acids to chelate with zinc ions, we first considered the spacing between the chelating group ('warhead') and the scaffold. In a strictly 2-dimensional sense, both captopril and CRATKML have a 2-carbon spacer between the sulfur and the carbonyl, whereas in the hydroxamic acids, there is only a one-atom spacer element. Therefore, our first analogs were designed to look at the difference in activity between 2-mercaptoacetamides versus 3-mercaptopropionamides. In the case of BoNT/A, we found that the enzyme prefers the one-carbon spacing found in the 2-mercaptoacetamides (for comparison, see analogs **7** vs **12a** in Table 1).

Having established an optimal positioning between the warhead and the scaffold, we then synthesized a focused library of 2-mercaptoacetamides,<sup>20–22</sup> which were screened against BoNT/A LC based on the assay developed by Schmidt.<sup>23–26</sup> Within this library we discovered a number of 'hit' structures, one of which was the simple 3-phenyl-1H-pyrazole-5-mercaptoacetamide (**4**, R = H). We focused our attention on this scaffold due to both its inherent drug-like properties as well as its amenability to chemical synthesis for rapid analoging. From our structure–activity relation-

ship (SAR) studies, we were able to develop this series into compounds that are equipotent<sup>27</sup> with Janda's hydroxamic acids. The mercaptoacetamides, however, show better cellular activity against the toxin.<sup>28</sup>

### 2.1. Chemistry

Each of the 2-mercaptoacetamides reported herein were prepared by heating thioglycolic acid with an appropriately substituted aminopyrazole at a concentration of 2 M in refluxing toluene under an atmosphere of argon. The reaction time for the amide formation step was found to be highly concentration dependent. In cases where the substituted phenylpyrazole was not commercially available, a synthetic route beginning with either the carboxylic acid, ester or  $\beta$ -ketonitrile precursor was utilized to synthesize the pyrazole (Scheme 1).

Compound **12a** was prepared in a four-step reaction sequence (Scheme 1) starting from commercially available 4-chlorobenzoic acid. The carboxylic acid was dissolved in methanol with a full equivalent of sulfuric acid and refluxed overnight to quantitatively yield the methyl ester. It should be noted that a catalytic amount of sulfuric acid was not sufficient to fully esterify the acid. The ester was then reacted with sodium methoxide in dry, refluxing acetonitrile to afford the  $\beta$ -ketonitrile. The nitrile was subsequently reacted with hydrazine to form the pyrazole heterocycle in good yield and purity.<sup>29</sup> We found that optimum purity and yields were realized by first reacting the hydrazine with the ketone at room temperature to form the hydrazone intermediate, followed by heating to promote intramolecular cyclization. The aminopyrazole was then treated with thioglycolic acid in the usual manner to provide the desired 2-mercaptoacetamide.

Compound **12b** was prepared in a three-step reaction pathway starting from the appropriately substituted, commercially available methyl ester (Scheme 1). As described above, the ester was reacted with acetonitrile/sodium methoxide to give the  $\beta$ -ketonitrile, which was subsequently cyclized with hydrazine. The resulting aminopyrazole was then reacted with thioglycolic acid in the usual manner to give compound **12b**.

Compounds **12c** and **12d** were synthesized in a two-step reaction sequence (Scheme 1) from their commercially available  $\beta$ -ketonitriles, which were subsequently reacted with hydrazine, and the resulting pyrazole then reacted with thioglycolic acid (vide supra).

The non-2-mercaptoacetamide analogs (**5**, **6**, and **7**) were prepared by amidation with their appropriate carboxylic acid. 5-Amino-3-(4-chlorophenyl)-pyrazole was reacted with 3-mercaptopropionic acid, glycolic acid and acetic acid respectively in toluene at 110 °C under argon to provide compounds **5**, **6**, and **7**.

### 2.2. Biological data and structure–activity relationship studies

To investigate our hypothesis that the mercaptoacetamide was forming a chelate with the zinc ion, we first explored amide-analogs of the 5-amino-3-(4-chlorophenyl)-pyrazole (Table 1). Both the presence of the sulfur atom and its position in the molecule are critical to the inhibitory action of these analogs. The 3-mercaptopropionamide analog (**5**) has only weak inhibitory activity (195  $\mu$ M), while the corresponding 2-mercaptoacetamide (**12a**) was shown to be significantly (40 $\times$ ) more potent with an  $IC_{50}$  of 4.8  $\mu$ M. Removal of the thiol group (**7**) or replacing it with a hydroxyl group (**6**) abolishes all activity. Given the extreme sensitivity to both the presence and positioning of the sulfur in these analogs, it is reasonable to assume that the sulfur's coordination with the zinc ion in the BoNT/A LC's active site is required for inhibition. This hypothesis was later verified using protein/small-molecule X-ray crystallographic studies.<sup>30</sup>

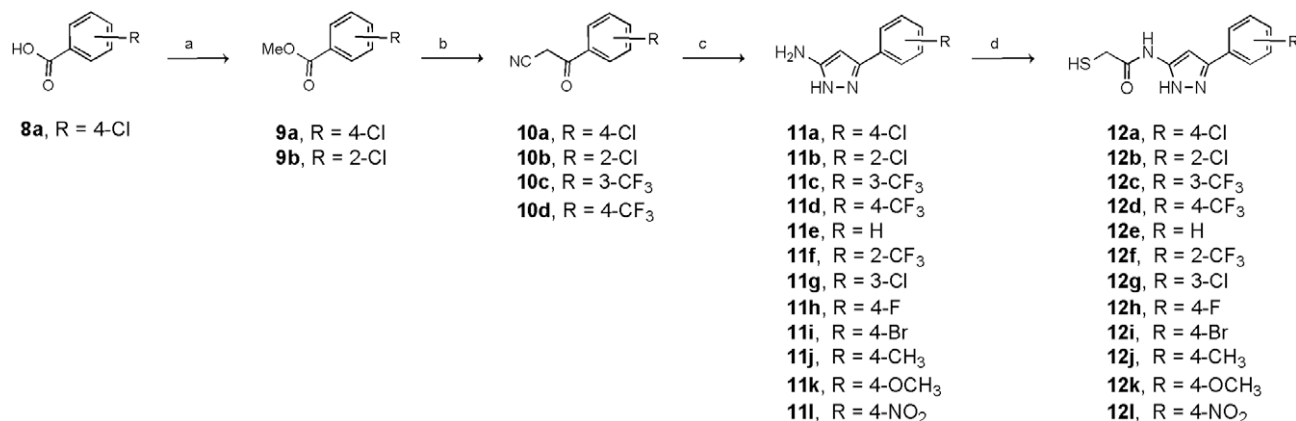
**Table 1**  
Relative position and importance of the thiol-SH

| Structure | Compound   | $IC_{50}$ ( $\mu$ M) BoNT/A <sup>a</sup> |
|-----------|------------|--|
|           | <b>5</b>   | 195 $\pm$ 93 <sup>b</sup>                |
|           | <b>12a</b> | 4.8 $\pm$ 1.3                            |
|           | <b>6</b>   | N.A. <sup>c</sup>                        |
|           | <b>7</b>   | N.A.                                     |

<sup>a</sup> BoNT/A wild-type length-425 with the 17-mer peptide substrate.

<sup>b</sup> Data represent the average value  $\pm$  SD of at least 3 experiments.

<sup>c</sup> N.A. (not active) is defined as <10% inhibition @ 50  $\mu$ M.



**Scheme 1.** Synthesis of 2-mercaptoacetamide analogs of 3-amino-5-phenylpyrazole. Reagents and conditions: (a) MeOH, H<sub>2</sub>SO<sub>4</sub>, reflux; (b) CH<sub>3</sub>CN, NaOMe; (c) NH<sub>2</sub>NH<sub>2</sub>, EtOH, rt to reflux; (d) HSCH<sub>2</sub>CO<sub>2</sub>H, toluene, 110 °C.

We next turned our attention to substituents on the phenyl ring to explore the effects on enzyme inhibition, and the results are shown in Tables 2 and 3. Table 2 shows a comparison of *para*-substituted phenyl ring analogs. The unsubstituted analog (**12e**) has an IC<sub>50</sub> of 14.5 μM. Substituting the ring in the 4-position with F (**12h**), Cl (**12a**), Br (**12i**), CF<sub>3</sub> (**12d**) or NO<sub>2</sub> (**12l**) gave more potent analogs, while the 4-Me (**12j**) and 4-OMe analogs (**12k**) were less active than the unsubstituted parent compound. The most pharmaceutically useful compounds in this series are **12a** and **12d**; the 4-Cl and 4-CF<sub>3</sub> analogs, respectively. Although the bromo (**12i**) and nitro (**12l**) analogs were essentially as potent as the 4-chloro, we did not follow up on these leads because these func-

tional groups pose challenges in drug development and have been associated with undesirable side effects and toxicity.<sup>31</sup>

We then looked at moving the chloro and trifluoromethyl substituents around the ring (Table 3). Interestingly, for either substituent there is essentially no difference in activity between the 3 and 4 position, both analogs show equipotency in either the *meta* or *para* positions. However, it was found that for the trifluoromethyl group, the *ortho* position yielded the greatest activity with an IC<sub>50</sub> of 7.2 μM (**12f**), while chlorine in the *para* position yielded the greatest activity, with an IC<sub>50</sub> of 4.8 μM (**12a**).

There are three interesting findings from these results. First, the active site of the enzyme does not seem to discriminate between the 3 or 4 positions. Apparently, as long as there is a bulky, electron-withdrawing substituent present in either of these positions, an increase in activity is realized relative to the unsubstituted aromatic ring. Second, in the specific examples of chloro and trifluoromethyl, the positions of the two substituents do not appear to produce similar effects on potency. While the 4-chloro analog (**12a**) is the most potent in the chlorine series, it was the 2-trifluoromethyl analog (**12f**) that showed the greatest activity within the trifluoromethyl series. At present, we have no explanation for these findings but speculate that it may have to do with the ability of fluorine atoms to participate in H-bonding. Finally, it is worth noting that the 2-chloro analog was actually less potent than having no substitution on the ring (**12b** vs **12e**). This is most interesting in light of the findings from the trifluoromethyl substituent and would clearly rule out some steric effect of the chlorine at this position.

### 3. Conclusion

Botulinum, a Class A pathogen, has the potential to cause devastation if used in a bio-terrorist attack. The difficulty in producing large quantities of antibody, the narrow window of opportunity for using an antibody and the lack of sufficient ventilators in case of an outbreak all point to the urgent need for therapeutic agents to combat this toxin. To this end, our group has focused on the development of small-molecule inhibitors against the LC-component of the toxin, and report herein the discovery and development of a novel series of mercaptoacetamido-phenylpyrazoles that show potent activity against the enzyme.

Preliminary SAR studies show that the presence and exact positioning of the sulfur atom in the warhead is essential for conferring activity. Additionally, at least within these analogs, BoNT/A does not discriminate between substitutions at the 3 or 4 position of the aromatic ring. The active site appears able to accommodate

**Table 2**  
Structure–activity studies: 4-substituted phenylpyrazoles

| Compound   | R                | IC <sub>50</sub> (μM) BoNT/A <sup>a</sup> |
|------------|------------------|---|
| <b>12e</b> | H                | 14.5 ± 0.7 <sup>b</sup>                   |
| <b>12h</b> | F                | 13.5 ± 4.9                                |
| <b>12a</b> | Cl               | 4.8 ± 1.3                                 |
| <b>12i</b> | Br               | 6.6 ± 0.6                                 |
| <b>12d</b> | CF <sub>3</sub>  | 10.0 ± 1.0                                |
| <b>12l</b> | NO <sub>2</sub>  | 2.9 ± 0.4                                 |
| <b>12j</b> | CH <sub>3</sub>  | 21.0 ± 2.5                                |
| <b>12k</b> | OCH <sub>3</sub> | 74.5 ± 2.1                                |

<sup>a</sup> BoNT/A wild-type length-425 with the 17-mer peptide substrate.

<sup>b</sup> Data represent the average value ± SD of at least 3 experiments.

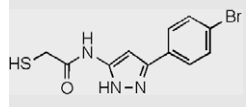
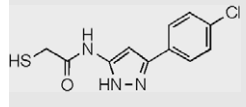
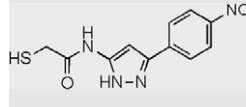
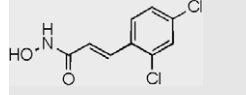
**Table 3**  
Structure–activity studies: position of ring substituents

| Compound   | R                 | IC <sub>50</sub> (μM) BoNT/A <sup>a</sup> |
|------------|-------------------|---|
| <b>12b</b> | 2-Cl              | 26.0 ± 2.8 <sup>b</sup>                   |
| <b>12g</b> | 3-Cl              | 5.6 ± 0.2                                 |
| <b>12a</b> | 4-Cl              | 4.8 ± 1.3                                 |
| <b>12f</b> | 2-CF <sub>3</sub> | 7.2 ± 0.7                                 |
| <b>12c</b> | 3-CF <sub>3</sub> | 13.0 ± 1.4                                |
| <b>12d</b> | 4-CF <sub>3</sub> | 10.0 ± 1.0                                |

<sup>a</sup> BoNT/A wild-type length-425 with the 17-mer peptide substrate.

<sup>b</sup> Data represent the average value ± SD of at least 3 experiments.

**Table 4**  
Comparison of thioacetamides with literature compound **2**

| Structure   | Compound   | IC <sub>50</sub> (μM) BoNT/A <sup>a</sup> |
|---|------------|---|
|  | <b>12i</b> | 6.6 ± 0.6 <sup>b</sup>                    |
|  | <b>12a</b> | 4.8 ± 1.3                                 |
|  | <b>12l</b> | 2.9 ± 0.4                                 |
|  | <b>2</b>   | 2.4 ± 0.6                                 |

<sup>a</sup> BoNT/A wild-type length-425 with the 17-mer peptide substrate.

<sup>b</sup> Data represent the average value ± SD of at least 3 experiments.

bulky, electron-withdrawing substituents at either of these positions. One of the more interesting findings from the SAR is with the apparent dichotic effects of Cl and CF<sub>3</sub> substitution. In the case of chlorine, the most active analog is the 4-Cl (**12a**) while the 2-Cl analog (**12b**) gave a compound that was less active than the unsubstituted phenyl (**12e** vs **12b**). On the other hand, for the trifluoromethyl group, the most active analog is the 2-CF<sub>3</sub> (**12f**). Clearly, there are additional electronic and/or H-bonding effects between these inhibitors and the active site than revealed in these simple SAR studies and we hope to report on this in more detail in the future.

When tested side-by-side, under our assay conditions,<sup>32</sup> these analogs show equipotency to the hydroxamic acid inhibitor (Table 4) reported by Janda's group to be the most potent small-molecule inhibitor to date. However, our mercaptoacetamides also show potent activity in a cellular assay while the hydroxamic acid (**2**) is inactive or cytotoxic.<sup>28</sup> More importantly, these mercaptoacetamides are able to prevent SNARE cleavage in neuronal cells *without* the need for pre-incubation of the small molecule with the toxin. Further work with our analogs suggests that they show inhibitory activity in the rat hemidiaphragm (phrenic nerve) and the rat *extensor digitorum longus* (EDL) *ex vivo* animal models.<sup>33</sup> Taken together, the data indicate that these novel, mercaptoacetamide-based inhibitors represent viable lead structures for further development into pharmaceutically useful therapeutics against botulinum intoxication.

#### 4. Experimental

NMR data were collected on a Varian 400 MHz Unity Inova NMR. Chemical shifts are reported in ppm using TMS in CDCl<sub>3</sub> or DMSO-*d*<sub>6</sub> as internal standards. Mass spectrometry data were collected on a JEOL JMS-600 (FAB-MS, NBA/NaI matrix). Analytical HPLC data were collected on a Hewlett Packard 1090 Series II HPLC using the following parameters: flow rate: 1 mL/min; column: Phenomenex, Luna 5 μm reverse-phase C18 (50 × 4.6 mm); temperature: 40 °C. Spectral data were collected at 2 wavelengths: 220 and 254 nm. Trifluoroacetic acid (0.1% v/v) was added to both HPLC eluents. Gradient: 95% H<sub>2</sub>O/5% acetonitrile (CH<sub>3</sub>CN) (*t* = 0) → 95% H<sub>2</sub>O/5% CH<sub>3</sub>CN (*t* = 0.10 min) → 70% H<sub>2</sub>O/30% CH<sub>3</sub>CN (*t* = 1.50 min) → 100% CH<sub>3</sub>CN (*t* = 8.00 min) → 100% CH<sub>3</sub>CN (*t* = 9.50 min). TLC was

performed on AnalTech Uniplat<sup>®</sup> Silica Gel HLF 250 μm plates. All chemicals were obtained from Sigma–Aldrich (Milwaukee, WI), Alfa Aesar (Haverhill, MA), Rieke Metals (Lincoln, NE), and ACB Blocks (Moscow, Russia) and used as received. Solvents were used without further purification, except where specified. Dry solvents were stored over activated 3 Å molecular sieves prior to use. All reactions were performed under an atmosphere of argon unless otherwise noted. Reactions requiring elevated temperature were placed in capped, glass tubes and inserted into an aluminum block heater manufactured by Pierce Reacti-Therm, Rockford, IL.

#### 4.1. *N*-(3-(4-Chlorophenyl)-1*H*-pyrazol-5-yl)-3-mercaptopropionamide (**5**)

3-(4-Chlorophenyl)-1*H*-pyrazol-5-amine (194 mg, 1 mmol) was weighed into a clean, oven-dried vial. Toluene (1 mL) and 3-mercaptopropionic acid (520 μL, 4 mmol) were added and the vial was purged with argon, sealed, and heated to 110 °C in an aluminum block for 48 h. After cooling to room temperature, the product crystallized from the reaction mixture. The product was collected on fritted glass and washed successively with satd NaHCO<sub>3</sub> (2 × 5 mL), H<sub>2</sub>O (2 × 5 mL), 1 N HCl (2 × 5 mL) and diethyl ether (2 × 5 mL). After drying under high vacuum, 206.4 mg (73%) of the 3-mercaptopropionamide was obtained as a white powder. <sup>1</sup>H NMR (DMSO-*d*<sub>6</sub>) δ 1.71 (t, 1H, –SH), 2.73 (t, 2H, –CH<sub>2</sub>–), 2.88 (app. q, 2H, –CH<sub>2</sub>–), 6.75 (s, 1H, pyrazole-CH), 7.37 (d, 2H), 7.68 (d, 2H), 10.01 (s, 1H, –CONH–), 12.24 (s, 1H, pyrazole-NH); MS (FAB+), 304 [M+Na]<sup>+</sup>; HPLC: *t*<sub>R</sub> = 4.91 min.

#### 4.2. *N*-(3-(4-Chlorophenyl)-1*H*-pyrazol-5-yl)-2-hydroxyacetamide (**6**)

3-(4-Chlorophenyl)-1*H*-pyrazol-5-amine (194 mg, 1 mmol) was weighed into a clean, oven-dried vial. Toluene (1 mL) and glycolic acid (120 μL, 2 mmol) were added and the vial was purged with argon, sealed, and heated to 110 °C in an aluminum block for 48 h. After cooling to room temperature, the product crystallized from the reaction mixture. The product was collected on fritted glass and washed successively with satd NaHCO<sub>3</sub> (2 × 5 mL), H<sub>2</sub>O (2 × 5 mL), 1 N HCl (2 × 5 mL) and diethyl ether (2 × 5 mL). After drying under high vacuum, 250.6 mg (100%) of the 2-hydroxyacetamide was obtained as a white powder. <sup>1</sup>H NMR (DMSO-*d*<sub>6</sub>) δ 4.00 (s, 2H, –CH<sub>2</sub>–), 5.66 (s, 1H, –OH–), 6.88 (s, 1H, pyrazole-CH), 7.48 (d, 2H, *J* = 8 Hz), 7.75 (d, 2H, *J* = 8 Hz), 9.85 (s, 1H, –CONH–), 12.99 (s, 1H, pyrazole-NH); MS (FAB+), 274 [M+Na]<sup>+</sup>; HPLC: *t*<sub>R</sub> = 3.97 min.

#### 4.3. *N*-(3-(4-Chlorophenyl)-1*H*-pyrazol-5-yl)acetamide (**7**)

3-(4-Chlorophenyl)-1*H*-pyrazol-5-amine (1.0 g, 5.2 mmol) was weighed into a vial containing toluene (2 mL). Acetic acid (450 μL, 7.7 mmol) was then added. The reaction was stirred at 110 °C in an aluminum block for 18 h. The product crystallized upon cooling to room temperature. The product was collected on fritted glass and washed with satd NaHCO<sub>3</sub> (2 × 5 mL), H<sub>2</sub>O (2 × 5 mL), 1 N HCl (2 × 5 mL), and diethyl ether (2 × 5 mL) to afford 1.06 g (86%) of the desired product as white crystals. <sup>1</sup>H NMR (DMSO-*d*<sub>6</sub>) δ 2.01 (s, 3H, –CH<sub>3</sub>), 6.91 (s, 1H, pyrazole-CH), 7.51 (d, 2H, *J* = 8 Hz), 7.74 (d, 2H, *J* = 8 Hz), 10.44 (s, 1H, –CONH–), 12.86 (s, 1H, pyrazole-NH); MS (FAB+), 258 [M+Na]<sup>+</sup>, *m/z* 236 [M+H]<sup>+</sup>; HPLC *t*<sub>R</sub>: 4.17 min.

#### 4.4. Methyl 4-chlorobenzoate (**9a**)

4-Chlorobenzoic acid (**8a**, 20 g, 128 mmol) was dissolved in methanol (250 mL, 6.2 mol). Sulfuric acid (concn, 6.8 mL, 128 mmol) was added and the mixture was heated at reflux for

18 h. After cooling to room temperature the reaction was evaporated under vacuum to approximately 25 mL and the residue was neutralized with satd aq NaHCO<sub>3</sub> (250 mL). The product was then extracted with CH<sub>2</sub>Cl<sub>2</sub> (3 × 100 mL). The combined organic extracts were dried (Na<sub>2</sub>SO<sub>4</sub>) and evaporated in vacuo to afford methyl 4-chlorobenzoate (20.72 g, 95%) as white crystals. <sup>1</sup>H NMR (CDCl<sub>3</sub>) δ 3.93 (s, 3H, –CH<sub>3</sub>), 7.42 (d, 2H), 7.97 (d, 2H); HPLC: *t*<sub>R</sub> = 5.98 min.

#### 4.5. 3-(4-Chlorophenyl)-3-oxopropanenitrile (10a)

4-Chlorobenzoate (**9a**, 20.5 g, 121 mmol) was dissolved in dry acetonitrile (250 mL). Under argon, sodium methoxide (13.0 g, 242 mmol) was added and the reaction mixture was heated to reflux for 2 h. Upon cooling to room temperature H<sub>2</sub>O (200 mL) was added and the reaction mixture was washed with CH<sub>2</sub>Cl<sub>2</sub> (3 × 75 mL). The aqueous layer was adjusted to pH 8.0 using 10% aq citric acid and the product precipitated upon standing. The product was collected on fritted glass and dried in vacuo to yield 3-(4-chlorophenyl)-3-oxopropanenitrile (9.32 g, 43%) as white crystals. <sup>1</sup>H NMR (CDCl<sub>3</sub>) δ 4.07 (s, 2H, –CH<sub>2</sub>), 7.51 (d, 2H), 7.87 (d, 2H); MS (FAB+), 202 [M+Na]<sup>+</sup>; HPLC: *t*<sub>R</sub> = 4.96 min.

#### 4.6. 3-(4-Chlorophenyl)-1H-pyrazol-5-amine (11a)

3-(4-Chlorophenyl)-3-oxopropanenitrile (**10a**, 2.0 g, 11.2 mmol) was weighed into a vial. Absolute ethanol (5.2 mL) and hydrazine (421 μL, 13.4 mmol) were added. The reaction was stirred at room temperature for 1 h and then heated to reflux for an additional 1 h. Upon cooling to room temperature water (10 mL) was added and the product precipitated upon standing. The precipitate was collected on fritted glass and washed with water (2 × 5 mL) to afford 3-(4-chlorophenyl)-1H-pyrazole-5-amine (1.69 g, 78%) as white crystals. <sup>1</sup>H NMR (DMSO-*d*<sub>6</sub>) δ 4.92 (s, 2H, –NH<sub>2</sub>), 5.75 (s, 1H, pyrazole-CH), 7.40 (d, 2H), 7.66 (d, 2H), 11.77 (s, 1H, pyrazole-NH); MS (FAB+), 216 [M+Na]<sup>+</sup>, *m/z* 194 [M+H]<sup>+</sup>; HPLC: *t*<sub>R</sub> = 3.42 min.

#### 4.7. N-(3-(4-Chlorophenyl)-1H-pyrazol-5-yl)-2-mercaptoacetamide (12a)

3-(4-Chlorophenyl)-1H-pyrazole-5-amine (**11a**, 1.69 g, 8.7 mmol) was weighed into a clean, oven-dried vial. Toluene (4 mL) and thioglycolic acid (910 μL, 13.1 mmol) were added and the vial was purged with argon, sealed, and heated to 110 °C in an aluminum block for 48 h. After cooling to room temperature the product crystallized and was collected on fritted glass and washed successively with satd NaHCO<sub>3</sub> (2 × 5 mL), H<sub>2</sub>O (2 × 5 mL), 1 N HCl (2 × 5 mL) and diethyl ether (2 × 5 mL). After drying under high vacuum 2.09 g (90%) of the mercaptoacetamide was obtained as white crystals. <sup>1</sup>H NMR (DMSO-*d*<sub>6</sub>) δ 2.90 (t, 1H, –SH, *J* = 8 Hz), 3.29 (d, 2H, –CH<sub>2</sub>–, *J* = 8 Hz), 6.92 (s, 1H, pyrazole-CH), 7.50 (d, 2H, *J* = 8 Hz), 7.74 (d, 2H, *J* = 8 Hz), 10.59 (s, 1H, –CONH–), 12.93 (s, 1H, pyrazole-NH); MS (FAB+), 290 [M+Na]<sup>+</sup>, *m/z* 268 [M+H]<sup>+</sup>; HPLC: *t*<sub>R</sub> = 4.65 min.

#### 4.8. 3-(2-Chlorophenyl)-3-oxopropanenitrile (10b)

In a clean, oven-dried 500 mL 3-necked flask equipped with a magnetic stir bar, gas inlet and reflux condenser, methyl 2-chlorobenzoate (**9b**, 12 g, 70 mmol) was dissolved in 250 mL of dry acetonitrile. Under an atmosphere of argon, sodium methoxide (7.6 g, 140 mmol) was added and the reaction was heated to reflux for 2 h. The solution was allowed to cool to room temperature and H<sub>2</sub>O (200 mL) was added. The solution was washed with CH<sub>2</sub>Cl<sub>2</sub> (3 × 100 mL) and the aqueous layer was adjusted to pH 8 using 10% aq citric acid. The aqueous layer was extracted with CH<sub>2</sub>Cl<sub>2</sub> (3 × 100 mL) and the organic layer was dried (Na<sub>2</sub>SO<sub>4</sub>) and evapo-

rated in vacuo to give 5.95 g (47%) of the β-ketonitrile as a bright yellow powder. <sup>1</sup>H NMR (CDCl<sub>3</sub>) δ 4.15 (s, 2H, –CH<sub>2</sub>), 7.41 (m, 1H), 7.49 (m, 2H), 7.64 (m, 1H); MS (FAB+), 202 [M+Na]<sup>+</sup>; HPLC: *t*<sub>R</sub> = 4.59 min.

#### 4.9. 3-(2-Chlorophenyl)-1H-pyrazol-5-amine (11b)

3-(2-Chlorophenyl)-3-oxopropanenitrile (**10b**, 2 g, 11.2 mmol) was dissolved in absolute EtOH (5.2 mL). Hydrazine (421 μL, 13.4 mmol) was added dropwise and the solution was stirred at room temperature for 1 h and then heated to reflux for an additional 1 h. The reaction mixture was cooled to room temperature and cold H<sub>2</sub>O (5 mL) was added and the product precipitated. The product was collected on fritted glass, washed with cold H<sub>2</sub>O (2 × 5 mL) and dried under high vacuum to provide 280 mg (13% yield) of the aminopyrazole as a white powder. <sup>1</sup>H NMR (DMSO-*d*<sub>6</sub>) δ 3.72 (s, 2H, –NH<sub>2</sub>), 6.17 (s, 1H, pyrazole-CH), 7.31 (m, 1H), 7.46 (m, 2H), 7.58 (m, 1H); MS (FAB+), 216 [M+Na]<sup>+</sup>, *m/z* 194 [M+H]<sup>+</sup>; HPLC: *t*<sub>R</sub> = 3.18 min.

#### 4.10. N-(3-(2-Chlorophenyl)-1H-pyrazol-5-yl)-2-mercaptoacetamide (12b)

3-(2-Chlorophenyl)-1H-pyrazol-5-amine (**11b**, 280 mg, 1.5 mmol) was weighed into a clean, oven-dried vial. Dry toluene (750 μL) and thioglycolic acid (151 μL, 2.2 mmol) were added. The vial was purged with argon, sealed, and heated to 110 °C in an aluminum block for 18 h. After cooling to room temperature, the product crystallized out of the reaction mixture. The product was collected on fritted glass and washed successively with satd NaHCO<sub>3</sub> (2 × 5 mL), H<sub>2</sub>O (2 × 5 mL), 1 N HCl (2 × 5 mL) and diethyl ether (2 × 5 mL). After drying under high vacuum, 223 mg (55%) of the mercaptoacetamide was obtained as a white powder. <sup>1</sup>H NMR (DMSO-*d*<sub>6</sub>) δ 2.90 (t, 1H, –SH, *J* = 8 Hz), 3.30 (d, 2H, –CH<sub>2</sub>–, *J* = 8 Hz), 6.89 (s, 1H, pyrazole-CH), 7.42 (m, 2H), 7.58 (dd, 2H, *J* = 8 Hz), 7.63 (dd, 1H, *J* = 8 Hz), 10.63 (s, 1H, –CONH–), 12.78 (s, 1H, pyrazole-NH); MS (FAB+), 290 [M+Na]<sup>+</sup>, *m/z* 268 [M+H]<sup>+</sup>; HPLC: *t*<sub>R</sub> = 4.33 min.

#### 4.11. 3-(3-(Trifluoromethyl)phenyl)-1H-pyrazol-5-amine (11c)

3-Oxo-3-(3-(trifluoromethyl)phenyl)propanenitrile (**10c**, 2.5 g, 11.7 mmol) was dissolved in absolute ethanol (5.0 mL). Anhydrous hydrazine (442 μL, 14 mmol) was added dropwise and the solution was stirred at room temperature for 1 h after which the reaction was heated to reflux for an additional 1 h. The reaction mixture was cooled to room temperature and cold H<sub>2</sub>O (5 mL) was added until the product precipitated. The product was collected on fritted glass, washed with cold H<sub>2</sub>O (2 × 5 mL) and dried under high vacuum to provide 2.20 g (82%) of the desired β-ketonitrile as an off-white powder. HPLC: *t*<sub>R</sub> = 3.73 min.

#### 4.12. N-(3-(3-(Trifluoromethyl)phenyl)-1H-pyrazol-5-yl)-2-mercaptoacetamide (12c)

3-(3-(Trifluoromethyl)phenyl)-1H-pyrazol-5-amine (**11c**, 2.20 g, 9.6 mmol) was weighed into a clean, oven-dried vial. Dry toluene (3.5 mL) and thioglycolic acid (1.0 mL, 14.5 mmol) were added and the vial was purged with argon, sealed, and heated to 110 °C in an aluminum block for 18 h. After cooling to room temperature, the product crystallized from the reaction mixture. The product was collected on fritted glass and washed successively with satd NaHCO<sub>3</sub> (2 × 5 mL), H<sub>2</sub>O (2 × 5 mL), 1 N HCl (2 × 5 mL) and diethyl ether (2 × 5 mL). After drying under high vacuum, 1.31 g (45%) of the 2-mercaptoacetamide was obtained as a white powder. <sup>1</sup>H NMR (DMSO-*d*<sub>6</sub>) δ 2.91 (t, 1H, –SH, *J* = 8 Hz), 3.30 (d, 2H, –CH<sub>2</sub>–,



$J = 8$  Hz), 7.02 (s, 1H, pyrazole-CH), 7.65–7.70 (m, 2H), 8.02–8.04 (m, 1H), 8.10 (s, 1H), 10.65 (s, 1H, –CONH–), 13.09 (s, 1H, pyrazole-NH); MS (FAB+), 324 [M+Na]<sup>+</sup>,  $m/z$  302 [M+H]<sup>+</sup>; HPLC:  $t_R = 5.04$  min.

#### 4.13. 3-(4-(Trifluoromethyl)phenyl)-1H-pyrazol-5-amine (11d)

3-Oxo-3-(4-(trifluoromethyl)phenyl)propanenitrile (**10d**, 2.0 g, 9.3 mmol) was dissolved in absolute ethanol (4.4 mL). Anhydrous hydrazine (344  $\mu$ L, 11.3 mmol) was added dropwise and the solution was stirred at room temperature for 1 h and then heated to reflux for an additional 1 h. The reaction mixture was cooled to room temperature and cold H<sub>2</sub>O (4 mL) was added until the product precipitated. The product was collected on fritted glass, washed with cold H<sub>2</sub>O (2  $\times$  5 mL) and dried under high vacuum to provide 1.89 g (90%) of the desired  $\beta$ -ketonitrile as an off-white powder. HPLC:  $t_R = 3.77$  min.

#### 4.14. N-(3-(4-(Trifluoromethyl)phenyl)-1H-pyrazol-5-yl)-2-mercaptoacetamide (12d)

3-(4-(Trifluoromethyl)phenyl)-1H-pyrazol-5-amine (**11d**, 1.89 g, 8.3 mmol) was weighed into a clean, oven-dried vial. Dry toluene (3.3 mL) and thioglycolic acid (870  $\mu$ L, 12.5 mmol) were added and the vial was purged with argon, sealed, and heated to 110 °C in an aluminum block for 18 h. After cooling to room temperature, the product crystallized from the reaction mixture. The product was collected on fritted glass and washed successively with satd NaHCO<sub>3</sub> (2  $\times$  5 mL), H<sub>2</sub>O (2  $\times$  5 mL), 1 N HCl (2  $\times$  5 mL) and diethyl ether (2  $\times$  5 mL). After drying under high vacuum, 2.04 g (82%) of the 2-mercaptoacetamide was obtained as a white powder. <sup>1</sup>H NMR (DMSO-*d*<sub>6</sub>)  $\delta$  2.90 (t, 1H, –SH,  $J = 8$  Hz), 3.30 (d, 2H, –CH<sub>2</sub>–,  $J = 8$  Hz), 7.04 (s, 1H, pyrazole-CH), 7.80 (d, 2H,  $J = 8$  Hz), 7.94 (d, 2H,  $J = 8$  Hz), 10.64 (s, 1H, –CONH–), 13.13 (s, 1H, pyrazole-NH); MS (FAB+), 324 [M+Na]<sup>+</sup>,  $m/z$  302 [M+H]<sup>+</sup>; HPLC:  $t_R = 5.09$  min.

#### 4.15. General method

The appropriately substituted aminopyrazole (2.0 mmol) was weighed into a clean, oven-dried vial. Thioglycolic acid (3.0 mmol) and dry toluene were added to give a final concentration of the aminopyrazole of 2 M. The vial was then purged with argon, sealed, and heated to 110 °C in an aluminum block heater/stirrer until the reaction was complete as determined by HPLC analysis (18–48 h). After cooling to room temperature, the product crystallized from the reaction mixture. Crystalline products were collected on fritted glass and washed successively with satd NaHCO<sub>3</sub> (2  $\times$  5 mL), H<sub>2</sub>O (2  $\times$  5 mL), 1 N HCl (2  $\times$  5 mL), and diethyl ether (2  $\times$  5 mL).

##### 4.15.1. N-(3-(Phenyl)-1H-pyrazol-5-yl)-2-mercaptoacetamide (12e)

In a similar manner as above, 3-phenyl-1H-pyrazol-5-amine (**11e**, 2.5 g, 15.7 mmol) was converted to the 2-mercaptoacetamide analog (2.98 g, 82%) as white crystals. <sup>1</sup>H NMR (DMSO-*d*<sub>6</sub>)  $\delta$  12.86 (s, 1H, pyrazole-NH), 10.58 (s, 1H, –CONH–), 7.72 (d, 2H,  $J = 7$  Hz), 7.45 (dd, 2H,  $J_1 = J_2 = 7$  Hz), 7.34 (dd, 1H,  $J_1 = J_2 = 7$  Hz), 6.87 (s, 1H, pyrazole-CH), 3.30 (d, 2H, –CH<sub>2</sub>–,  $J = 8$  Hz), 2.90 (t, 1H, –SH,  $J = 8$  Hz); MS (FAB+), 256 [M+Na]<sup>+</sup>,  $m/z$  234 [M+H]<sup>+</sup>; HPLC:  $t_R = 3.98$  min.

##### 4.15.2. N-(3-(2-(Trifluoromethyl)phenyl)-1H-pyrazol-5-yl)-2-mercaptoacetamide (12f)

In a similar manner as above, 3-(2-(trifluoromethyl)phenyl)-1H-pyrazol-5-amine (**11f**, 100 mg, 0.44 mmol) was converted to 45 mg (34%) of the 2-mercaptoacetamide as a white powder. <sup>1</sup>H NMR (DMSO-*d*<sub>6</sub>)  $\delta$  2.89 (t, 1H, –SH,  $J = 8$  Hz), 3.29 (d, 2H, –CH<sub>2</sub>–,  $J = 8$  Hz), 6.71 (s, 1H, pyrazole-CH), 7.59 (d, 1H,  $J = 8$  Hz), 7.66 (dd,

1H,  $J_1 = J_2 = 8$  Hz), 7.76 (dd, 1H,  $J_1 = J_2 = 8$  Hz), 7.86 (d, 1H,  $J = 8$  Hz), 10.61 (s, 1H, –CONH–), 12.72 (s, 1H, pyrazole-NH); MS (FAB+), 324 [M+Na]<sup>+</sup>,  $m/z$  302 [M+H]<sup>+</sup>; HPLC:  $t_R = 4.62$  min.

##### 4.15.3. N-(3-(3-Chlorophenyl)-1H-pyrazol-5-yl)-2-mercaptoacetamide (12g)

In a similar manner as above, 3-(3-chlorophenyl)-1H-pyrazol-5-amine (**11g**, 50 mg, 0.26 mmol) was converted to 68 mg (98%) of the 2-mercaptoacetamide as white crystals. <sup>1</sup>H NMR (DMSO-*d*<sub>6</sub>)  $\delta$  2.35 (br s, 1H, –SH), 3.35 (s, 2H, –CH<sub>2</sub>–), 6.83 (s, 1H, pyrazole-CH), 7.26–7.29 (m, 1H), 7.36 (dd, 1H,  $J_1 = J_2 = 8$  Hz), 7.60 (dd, 1H,  $J_1 = 8$  Hz,  $J_2 = 1$  Hz), 7.74 (dd, 1H,  $J_1 = J_2 = 2$  Hz), 10.96 (s, 1H, –CONH–), 12.15 (s, 1H, pyrazole-NH); MS (FAB+), 290 [M+Na]<sup>+</sup>; HPLC:  $t_R = 4.67$  min.

##### 4.15.4. N-(3-(4-Fluorophenyl)-1H-pyrazol-5-yl)-2-mercaptoacetamide (12h)

In a similar manner as above, 3-(4-fluorophenyl)-1H-pyrazol-5-amine (**11h**, 4.6 g, 26 mmol) was converted to 5.55 g (85%) of the 2-mercaptoacetamide as white crystals. <sup>1</sup>H NMR (DMSO-*d*<sub>6</sub>)  $\delta$  2.50 (br s, 1H, –SH), 3.30 (s, 2H, –CH<sub>2</sub>–), 6.88 (s, 1H, pyrazole-CH), 7.29 (dd, 2H,  $J_1 = J_2 = 8$  Hz), 7.77 (dd, 2H,  $J_1 = 8$  Hz,  $J_2 = 6$  Hz), 10.59 (s, 1H, –CONH–), 12.86 (s, 1H, pyrazole-NH); MS (FAB+), 274 [M+Na]<sup>+</sup>; HPLC:  $t_R = 4.08$  min.

##### 4.15.5. N-(3-(4-Bromophenyl)-1H-pyrazol-5-yl)-2-mercaptoacetamide (12i)

In a similar manner as above, 3-(4-bromophenyl)-1H-pyrazol-5-amine (**11i**, 238 mg, 1.0 mmol) was converted to 236 mg (76%) of the 2-mercaptoacetamide as white crystals. <sup>1</sup>H NMR (DMSO-*d*<sub>6</sub>)  $\delta$  2.88 (t, 1H, –SH,  $J = 8$  Hz), 3.28 (d, 2H, –CH<sub>2</sub>–,  $J = 8$  Hz), 6.87 (s, 1H, pyrazole-CH), 7.62 (d, 2H,  $J = 9$  Hz), 7.67 (d, 2H,  $J = 9$  Hz), 10.67 (s, 1H, –CONH–), 12.92 (s, 1H, pyrazole-NH); MS (FAB+), 334, 336 [M+Na]<sup>+</sup>; HPLC:  $t_R = 4.83$  min.

##### 4.15.6. N-(3-*p*-Tolyl-1H-pyrazol-5-yl)-2-mercaptoacetamide (12j)

In a similar manner as above, 3-*p*-tolyl-1H-pyrazol-5-amine (**11j**, 257 mg, 1.5 mmol) was converted to 315 mg (85%) of the 2-mercaptoacetamide as white crystals. <sup>1</sup>H NMR (DMSO-*d*<sub>6</sub>)  $\delta$  2.31 (s, 3H, –CH<sub>3</sub>), 2.88 (t, 1H, –SH,  $J = 8$  Hz), 3.29 (d, 2H, –CH<sub>2</sub>–,  $J = 8$  Hz), 6.83 (s, 1H, pyrazole-CH), 7.24 (d, 2H,  $J = 8$  Hz), 7.59 (d, 2H,  $J = 8$  Hz), 10.55 (s, 1H, –CONH–), 12.77 (s, 1H, pyrazole-NH); MS (FAB+), 270 [M+Na]<sup>+</sup>,  $m/z$  248 [M+H]<sup>+</sup>; HPLC:  $t_R = 4.44$  min.

##### 4.15.7. N-(3-(4-Methoxyphenyl)-1H-pyrazol-5-yl)-2-mercaptoacetamide (12k)

In a similar manner as above, 3-(4-methoxyphenyl)-1H-pyrazol-5-amine (**11k**, 568 mg, 3.0 mmol) was converted to 676 mg (86%) of the 2-mercaptoacetamide as white crystals. <sup>1</sup>H NMR (DMSO-*d*<sub>6</sub>)  $\delta$  2.89 (t, 1H, –SH,  $J = 8$  Hz), 3.29 (d, 2H, –CH<sub>2</sub>–,  $J = 8$  Hz), 3.79 (s, 3H, –CH<sub>3</sub>–), 6.77 (s, 1H, pyrazole-CH), 7.00 (d, 2H,  $J = 9$  Hz), 7.65 (d, 2H,  $J = 9$  Hz), 10.54 (s, 1H, –CONH–), 12.75 (s, 1H, pyrazole-NH); MS (FAB+), 286 [M+Na]<sup>+</sup>,  $m/z$  264 [M+H]<sup>+</sup>; HPLC:  $t_R = 3.98$  min.

##### 4.15.8. N-(3-(4-Nitrophenyl)-1H-pyrazol-5-yl)-2-mercaptoacetamide (12l)

In a similar manner as above, 3-(4-nitrophenyl)-1H-pyrazol-5-amine (**11l**, 1.0 g, 4.9 mmol) was converted to 1.32 g (97%) of the 2-mercaptoacetamide as yellow crystals. <sup>1</sup>H NMR (DMSO-*d*<sub>6</sub>)  $\delta$  2.92 (s, 1H, –SH), 3.31 (s, 2H, –CH<sub>2</sub>–), 7.12 (s, 1H, pyrazole-CH), 8.01 (d, 2H,  $J = 8$  Hz), 8.29 (d, 2H,  $J = 8$  Hz), 10.70 (s, 1H, –CONH–), 13.26 (s, 1H, pyrazole-NH); MS (FAB+), 301 [M+Na]<sup>+</sup>,  $m/z$  279 [M+H]<sup>+</sup>; HPLC:  $t_R = 4.28$  min.

#### 4.16. Biochemical assay

Numerous assays have been developed for testing analogs for inhibitory activity against botulinum toxin. The compounds in this manuscript were tested for ability to inhibit botulinum toxin in the enzyme assay as developed by Schmidt et al.<sup>23–25,34</sup>

##### 4.16.1. Construction of botulinum light chain protease truncation variants

A synthetic C-terminal truncation variant (1–425) of BoNTA-LC was created by standard molecular biology techniques. This variant was first reported by Barbieri to possess improved solubility properties over the wild-type WT enzyme while maintaining significant enzymatic activity.<sup>35</sup> Briefly, a doubly His-tagged BoNTA-LC cDNA sequence inserted in pET-14b plasmid vector (kindly provided by Dr. Charles Shoemaker, Tufts University) was modified via site-directed mutagenesis (QuikChange, Stratagene, La Jolla, CA) to introduce a stop codon designed to excise the C-terminal His tag and create the C-terminal truncation after lysine 425. The subclone was verified by DNA sequence analysis prior to transformation of BL21 Gold *Escherichia coli* bacterial expression vector (Stratagene).

##### 4.16.2. Expression and purification of BoNTA-LC variants

*E. coli* clones expressing BoNTA-LC 1–425 were grown at 37 °C in 3 L ZB-M9 medium (1% N-Z-amine A/0.5% NaCl/0.3% KH<sub>2</sub>PO<sub>4</sub>/0.6% Na<sub>2</sub>HPO<sub>4</sub>/0.1% NH<sub>4</sub>Cl/0.4% glucose/1 mM MgSO<sub>4</sub>) cultures containing 100 µg/mL ampicillin to an OD<sub>600</sub> reading of 0.5–1.0 before induction of expression by introduction of 0.5 µM isopropyl-β-D-1-thiogalactopyranoside. Expression was carried out for 18 h at 18 °C, before the cells were harvested by centrifugation, resuspended in 20 mM HEPES/500 mM NaCl/10 mM Imidazole/1 mM PMSF/25 µg/mL DNase/pH 8.0, and lysed using a microfluidizer. Each lysate was immediately processed with a Zn-charged HiTrap IMAC HP (Amersham Biosciences, Piscataway, NJ) column equilibrated in 20 mM HEPES/500 mM NaCl/10 mM imidazole/pH 8.0. Bound protein was eluted in 20 mM HEPES/500 mM NaCl/250 mM imidazole/pH 8.0, and fractions of peak protein concentration were combined 1:1 with glycerol for storage at –20 °C. Homogeneity of each prep was assessed by SDS–PAGE and was found to be >95% BoNTA-LC.

##### 4.16.3. Peptide substrate derivatization

The SNAP-25-based fluorescent peptide substrate was generated by a procedure modified from the method of Schmidt<sup>23</sup> 50 mg of SNRTRIDEAN[2,4-dinitrophenyl-K]RACRML peptide (American Peptide Co, Sunnyvale, CA) was combined with 20 mg N-(7-dimethylamino-4-methylcoumarin-3-yl)iodoacetamide (DACAIA) (Invitrogen, Carlsbad, CA) in 3 mL DMSO (Sigma–Aldrich Corp., St. Louis, MO) and the reaction was incubated in the dark at rt for 2 h. Peptide derivatized at the cysteine residue was purified via an Oasis HLB cartridge (Waters Corporation, Milford, MA) and eluted in 50% MeOH/2% acetic acid. Peptide concentration was determined by 365-nm absorbance ( $\epsilon = 36,500 \text{ M}^{-1} \text{ cm}^{-1}$ ) and peptide homogeneity was confirmed by reversed-phase HPLC using free and derivatized peptide standards.

##### 4.16.4. In vitro assessment of peptide substrate cleavage by BoNTA-LC

The assay utilized in these studies was originally developed by Schmidt.<sup>23</sup> Reactions between recombinant BoNTA-LC and fluorescent peptide substrate described above were carried out in 40 mM HEPES/pH 7.4 at rt, in a total volume of 200 µL in 96-well microplates. Substrate concentration in each reaction was 10 µM and enzyme concentration was 200 nM. Reaction progress was measured continuously by increase in fluorescence at Ex = 398 nm, Em =

485 nm (Gemini XPS fluorescence plate reader, Molecular Devices Corp., Sunnyvale, CA) as the cleavage of the substrate relieved the quenching of DACAIA fluorescence by the 2,4-dinitrophenyl-lysine. For inhibitor evaluation, compounds were added to each reaction from 100× DMSO stocks at each tested concentration to yield a final DMSO concentration of 1%. Control rates were measured in the presence of 1% DMSO. For each assessment, enzyme and inhibitor were pre-incubated for 30 min at rt before initiation of the reaction by substrate addition.

##### 4.16.5. IC<sub>50</sub> calculations

The initial velocity values for BoNTA-LC enzymatic cleavage of peptide substrate, recorded in the presence of 1% DMSO or one of a series of inhibitor concentrations, were plotted against inhibitor concentration. Each initial velocity value plotted represented the average of at least two reactions at each inhibitor concentration. The points were then fit to the following equation by non-linear regression analysis using the graphing program Prism (GraphPad Software, La Jolla, CA):

$$Y = \text{Bottom} + (\text{Top} - \text{Bottom}) / (1 + (X / \text{IC}_{50})^n)$$

where Y is the initial reaction velocity, Top is the upper asymptote of the resulting sigmoidal curve and Bottom is the lower asymptote, X is the concentration of inhibitor corresponding to the initial velocity Y, IC<sub>50</sub> is the inhibitor concentration that achieves half-maximal enzyme inhibition, and n is the Hill coefficient for the curve (a measure of cooperativity of ligand binding). Reported potency values for each compound represent the average of at least two independent determinations, and are expressed in terms of IC<sub>50</sub> because of the lack of mechanistic information for the complete set of compounds. Similar compounds with zinc-binding moieties have been demonstrated to bind in the active site of BoNTA-LC<sup>36</sup> and therefore are likely to act as competitive inhibitors. This report and the fact that the peptide substrate is used at a concentration well below its K<sub>m</sub> for BoNTA-LC (100 µM, see Schmidt<sup>23</sup>) predict that IC<sub>50</sub> is roughly equivalent to K<sub>i</sub> for this class of inhibitors, given that for competitive inhibitors  $K_i = \text{IC}_{50} / (1 + S / K_m)$ , where S is the initial substrate concentration in the reaction.

#### Acknowledgments

The authors are grateful to Dr. Tun-Li Shen of Brown University, Providence, RI for performing mass spectral analyses and Dr. Jin Hong and Alison Gallagher of Custom NMR Services, Ayer, MA for providing our group with NMR data. We thank Professor Saul Tzipori and Tufts University School of Veterinary Medicine Grafton, MA for their support in this work. This project has been funded in whole or in part with Federal funds from the Food and Waterborne Diseases Integrated Research Network (FWD IRN), the National Institute of Allergy and Infectious Diseases (NIAID), National Institutes of Health (NIH) and the United States Department of Health and Human Services (DHHS) under Contract No. N01-AI-30050.

#### References and notes

- Schantz, E. J.; Johnson, E. A. *Microbiol. Rev.* **1992**, *56*, 80.
- Singh, B. R. *Nat. Struct. Biol.* **2000**, *7*, 617.
- Arnon, S. S.; Schechter, R.; Inglesby, T. V.; Henderson, D. A.; Bartlett, J. G.; Ascher, M. S.; Eitzen, E.; Fine, A. D.; Hauer, J.; Layton, M.; Lillibridge, S.; Osterholm, M. T.; O'Toole, T.; Parker, G.; Perl, T. M.; Russell, P. K.; Swerdlow, D. L.; Tonat, K. *J. Am. Med. Assoc.* **2001**, *285*, 1059.
- Osborne, S. L.; Latham, C. F.; Wen, P. J.; Cavaignac, S.; Fanning, J.; Foran, P. G.; Meunier, F. A. *J. Neurosci. Res.* **2007**, *85*, 1149.
- For a review of botulinum neurotoxins see: Willis, B.; Eubanks, L. M.; Dickerson, T. J.; Janda, K. D. *Angew. Chem., Int. Ed.* **2008**, *47*, 8360.
- Montecucco, C. *Trends Biochem. Sci.* **1986**, *11*, 314.
- Schiavo, G.; Matteoli, M.; Montecucco, C. *Physiol. Rev.* **2000**, *80*, 717.

8. Simpson, L. L. *Annu. Rev. Pharmacol. Toxicol.* **2004**, 44, 167.
9. Rosenbloom, M.; Leikin, J. B.; Vogel, S. N.; Chaudry, Z. A. *Am. J. Therap.* **2002**, 9, 5.
10. Schmidt, J. J.; Stafford, R. G.; Bostian, K. A. *FEBS Lett.* **1998**, 435, 61.
11. Schmidt, J. J.; Stafford, R. G. *FEBS Lett.* **2002**, 532, 423.
12. Oost, T.; Sukonpan, C.; Brewer, M.; Goodnough, M.; Tepp, W.; Johnson, E. A.; Rich, D. H. *Biopolymers* **2003**, 71, 602.
13. Brewer, M.; James, C. A.; Rich, D. H. *Org. Lett.* **2004**, 6, 4779.
14. Haug, B. E.; Rich, D. H. *Org. Lett.* **2004**, 6, 4783.
15. Sukonpan, C.; Oost, T.; Goodnough, M.; Tepp, W.; Johnson, E. A.; Rich, D. H. *J. Pept. Res.* **2004**, 63, 181.
16. Monteucco, C.; Papini, E.; Schaivo, G. *FEBS Lett.* **1994**, 346, 92.
17. Boldt, G. E.; Kennedy, J. P.; Janda, K. D. *Org. Lett.* **2006**, 8, 1729.
18. Capková, K.; Yoneda, Y.; Dickerson, T. J.; Janda, K. D. *Bioorg. Med. Chem. Lett.* **2007**, 17, 6463.
19. Natesh, R.; Schwager, S. L.; Evans, H. R.; Sturrock, E. D.; Acharya, K. R. *Biochem.* **2004**, 43, 8718.
20. Moe, S. T.; Jacobson, A. J. U.S. Patent Pending, 2007.
21. Moe, S.; Smith, G.; Thompson, A.; Fredenburg, R.; Stein, R.; Park, J.-B.; Tzipori, S.; Janda, K.; Silvaggi, N.; Allen, K.; Jacobson, A. 44th Annual Interagency Botulism Research Coordinating Committee (IBRCC), October 14–18, 2007; Asilomar, CA.
22. Moe, S. T.; Jacobson, A. J. U.S. Provisional Patent 61/1003,394, 2008.
23. Schmidt, J. J.; Stafford, R. G. *Appl. Environ. Microbiol.* **2003**, 69, 297.
24. Schmidt, J. J.; Bostian, K. A. *J. Protein Chem.* **1995**, 14, 703.
25. Schmidt, J. J.; Bostian, K. A. *J. Protein Chem.* **1997**, 16, 19.
26. Schmidt, J. J.; Stafford, R. G.; Millard, C. B. *Anal. Biochem.* **2001**, 296, 130.
27. Fredenburg, R. A.; Wilson, D.; Moe, S. T.; Jacobson, A. R.; Stein, R. L. 44th Annual Interagency Botulism Research Coordinating Committee (IBRCC); October 14–18, 2007, Asilomar, CA.
28. Lee, J. O.; Ramasamy, U.; Tzipori, S.; Moe, S. T.; Smith, G. M.; Jacobson, A. R.; Park, J. B. 44th Annual Interagency Botulism Research Coordinating Committee (IBRCC); October 14–18, 2007; Asilomar, CA.
29. Endo, Y.; Fujishima, H.; Murai, K.; Miyata, T.; Wakisaka, S.; Sasama, Y. U.S. Patent 5,739,083, April 14, 1998.
30. Allen, K. N. Boston University, private communication.
31. May, P. In *The Chemistry of Synthetic Drugs*, 2nd ed.; Longmans, Green: London, 1918; pp 23–25.
32. The assay we employed utilized a form of the LC which did not have any mutations and was truncated at position 425. Although the C-terminus is not believed to be involved in the catalytic machinery of the enzyme, it has been observed (see Ref. 27) that the exact truncation point can effect measured IC<sub>50</sub> values and likely accounts for the difference in the IC<sub>50</sub> value of the hydroxamate (2) to that reported (Refs. 17 and 18).
33. Adler, M.; Aplan, J. P.; Ternay, A.; Janda, K.; Deshpande, S. S. 44th Annual Interagency Botulism Research Coordinating Committee (IBRCC); October 14–18, 2007; Asilomar, CA.
34. Boldt, G. E.; Kennedy, J. P.; Hixon, M. S.; McAllister, L. A.; Barbieri, J. T.; Tzipori, S.; Janda, K. D. *J. Comb. Chem.* **2006**, 8, 513.
35. Baldwin, M. R.; Bradshaw, M.; Johnson, E. A.; Barbieri, J. T. *Protein Expression Purif.* **2004**, 37, 187.
36. Silvaggi, N. R.; Boldt, G. E.; Hixon, M. S.; Kennedy, J. P.; Tzipori, S.; Janda, K. D.; Allen, K. N. *Chem. Biol.* **2007**, 14, 533.